International Journal of Adhesion & Adhesives 59 (2015) 77–85

Contents lists available at ScienceDirect

International Journal of Adhesion & Adhesives

journal homepage: www.elsevier.com/locate/ijadhadh

Monitoring the early stiffness development in epoxy adhesives for structural strengthening

José L. Granja, Pedro Fernandes, Andrea Benedetti, Miguel Azenha, José Sena-Cruz *

ISISE – Institute for Sustainability and Innovation in Structural Engineering, University of Minho, School of Engineering, Department of Civil Engineering, Campus de Azurém, 4800-058 Guimarães, Portugal

ARTICLE INFO

Article history:
Accepted 10 February 2015
Available online 23 February 2015

Keywords:
A. Epoxy/epoxides
C. Non-destructive testing
D. Cure/hardening
D. Elastic modulus
Cyclic tensile test

ABSTRACT

The present work aimed to assess the early-age evolution of *E*-modulus of epoxy adhesives used for Fibre-Reinforced Polymer (FRP) strengthening applications. The study involved adapting an existing technique devised for continuous monitoring of concrete stiffness since casting, called EMM-ARM (Elasticity Modulus Measurement through Ambient Response Method) for evaluation of epoxy stiffness. Furthermore, monotonic tensile tests according to ISO standards and cyclic tensile tests were carried out at several ages. A comparison between the obtained results was performed in order to better understand the performance of the several techniques in the assessment of stiffness of epoxy resins. When compared to the other methodologies, the method for calculation of *E*-modulus recommended by ISO standard led to lower values, since in the considered strain interval, the adhesive had a non-linear stress–strain relationship. The EMM-ARM technique revealed its capability in clearly identifying the hardening kinetics of epoxy adhesives, measuring the material stiffness growth during the entire curing period. At very early ages the values of Young's modulus obtained with quasi-static tests were lower than the values collected by EMM-ARM, due to the fact that epoxy resin exhibited a significant visco-elastic behaviour.

1. Introduction

In recent years, the application of thermosetting resins in civil engineering applications has largely increased, mainly for their use in structural strengthening systems such as Fibre-Reinforced Polymer (FRP) reinforcements [1]. The most common resins employed as structural adhesive for bonding FRP to structural elements to be strengthened are two-component epoxy resins [2,3].

In FRP installations, the mechanical behaviour of the strengthening system is strongly influenced by the epoxy adhesive, particularly at early ages, while the mechanical properties of the adhesive are still enduring significant evolution. Therefore, the final performance of the whole application strongly depends on adequate preparation, application and curing of the epoxy resin itself. During the curing period, the fluid resin transforms into a rubber (gelation) and then in a solid glass (vitrification), developing a progressively denser polymeric network [4].

It has been shown that the necessary curing time to reach the targeted bond strength of a given resin significantly depends on environmental conditions, such as temperature and moisture [5,6]. Lapique et al. [7] and Moussa et al. [8] have investigated the effect of the curing temperature on the development of the mechanical properties of epoxy resins generally utilized for structural strengthening, reaching similar conclusions: as both time and temperature increase, the epoxy tensile strength increases. Additionally, adhesives used for FRP strengthening applications must cure in-situ at various environmental conditions.

From the above considerations, it is clear that the development and implementation of non-destructive methods that are able to provide continuous information correlated to the curing process of epoxy resins are of paramount importance for in-situ applications of strengthening systems. The determination of the time at which the material becomes actually capable of bearing structurally relevant stresses is fundamental (and especially important in the case of pre-stressed systems [9]), as well as the stiffness increase along time. In fact, the elasticity modulus (*E*-modulus) of a polymer material such as cured epoxy adhesive is one of the most significant material parameters in structural analysis. Usually *E*-modulus values are obtained from tensile mechanical tests under a monotonic state of stress and there are already available several standards (e.g. ISO 527-1:2012 and ASTM D638M-93). It is nonetheless remarked that some of these standards are specifically directed to secant *E*-modulus, and do not take into account the strength of the material in the testing/calculation

* Corresponding author. Tel.: +351 253 510 200; fax: +351 253 510 217.
E-mail address: jsena@civil.uminho.pt (J. Sena-Cruz).

http://dx.doi.org/10.1016/j.ijadhadh.2015.02.005
0143-7496/

procedure. Additionally, tensile tests can solely provide measurements at discrete instants and they are complicated to perform on the construction site (most of the times due to economical unfeasibility).

For the aforementioned reasons, alternative vibration-based techniques are commonly utilized nowadays for the study of polymer-based plastic materials. The most widely used vibration-based techniques for *E*-modulus determination are the resonant frequency-based methods [10], as well as the dynamic mechanical analysis (DMA) [11]. Both these methods require the application of a mechanical force and therefore it is clear that these techniques are only suitable for specimens which have developed enough stiffness at the age of testing. Moreover, there are reports that the elastic modulus values obtained from DMA show large discrepancies between specimens and are in many cases different from those measured by quasi-static mechanical tests, as can be seen in the paper of Deng et al. [11]. Another promising dynamic test method is the novel torsion pendulum test developed by Yu et al. [12]. This technique allows measuring the dynamic shear modulus of adhesives since the early stages of the cure, monitoring the change of the resonant frequency with time.

Alternatively, techniques based on the propagation of ultrasonic waves through the sample can provide continuous measurement of the elasticity modulus of composite materials, ranging from the fluid-like stage up to the fully hardened state [13]. Even though these wave-based methods allow overcoming some of the drawbacks of the conventional techniques based on the resonance frequency, there are relatively frequent problems in the interpretation of the signals, and some of the basic assumptions for the interpretation of results (e.g. the tested material should be homogeneous and isotropic) are jeopardized when applied to a composite material as the case of epoxy resin [14].

Azenha et al. [15] proposed a novel method to measure *E*-modulus evolution in concrete, called Elasticity Modulus Measurement through Ambient Response Method (EMM-ARM). The method is based on the direct measurement of the evolution of the natural frequency of vibration of a composite beam, filled with the material under testing. The evolving natural frequency of the composite beam can thus be directly converted into the *E*-modulus of the tested material, based on the dynamic equations of motion of the system. The method allows continuous concrete *E*-modulus measurements immediately after casting and was applied also to identify the elastic modulus evolution of cement pastes, mortars and stabilized soils [16].

The present work aimed to study the early-age evolution of *E*-modulus of epoxy materials used for FRP applications, and better understand the relationship between distinct approaches for its assessment. For this purpose, a simultaneous study of *E*-modulus of the same adhesive mixture was carried out through EMM-ARM, together with tensile testing according to ISO standards (monotonic secant *E*-modulus) at several ages. Furthermore, since no publications were found in literature related to the inter-comparison of the epoxy *E*-modulus by means of monotonic tensile tests (such as the case of the ISO standard) and cyclic tensile tests, specific experiments were performed in such concern. Overall, this research work assists clarifications about the applicability of several approaches/techniques in predicting the stiffness of epoxy resins.

2. Experimental programme

The experimental programme consisted in the execution of an epoxy resin mixture and the characterization of the corresponding stiffness evolution along the curing time by monotonic tensile tests (MTT), cyclic tensile tests (CTT) and EMM-ARM tests. The two-component epoxy resin-based adhesive used in the experimental work, produced by S&P® Clever Reinforcement, had the trademark 'S&P Resin 220 epoxy adhesive'. This adhesive is typically employed for bonding FRP laminates to concrete and steel, and therefore may be seen as representative. According to the manufacturer [17], the component A (resin) contains 20–25% (by weight) Bisphenol A-Epoxy Resin and 5–10% Neopentyl glycol diglycidyl ether and, the component B (hardener) includes 20–25% poly (oxypropylene) diamine, 1–2.5% piperazine and 20–25% 3,6-diazaoctanethylenediamin; triethylenetetramine. All the specimens tested in the scope of this research were originated from a single batch that involved a total volume of epoxy resin of ~1.2 l. The individual components were separately stirred and then component B was added to component A at a ratio of 1:4 by weight of the respective constituents. To minimize air inclusions, the compound was thoroughly and slowly manually mixed until the colour was uniformly grey and free of any streaks. The whole mixing procedure lasted approximately 4 min.

All experimental procedures (mixing and testing) took place under controlled environmental conditions (in climatic chamber), with temperature of 20 ± 1 °C and relative humidity of 55 ± 5%. The following sections detail the programme of tests, methods and the procedures of test series, including sample geometries, test configurations and preparation of specimens.

2.1. Tensile tests – MTT and CTT

An extensive set of 30 tensile tests were performed in order to determine the epoxy *E*-modulus at several ages.

The specimens for testing were manufactured according to "type 1A" defined in EN ISO 527-2:2012. This specimen's geometry is characterized by having a dog bone shape at both extremities, with a thickness of 4 mm and overall geometry defined as shown in Fig. 1. Teflon moulds were devised for fabrication of the specimens. After mixing the two resin components, the homogenized compound was cast into the referred Teflon moulds. Afterwards an acetate sheet was placed on the top surface and pressed with a steel roller. The specimens were kept sealed in the curing environment and were removed from the moulds just before being tested. For all specimens, width and thickness were measured at the three sections (S1, S2 and S3) identified in Fig. 1, using a digital calliper with a precision of ±0.01 mm, to check tolerances and for longitudinal stress calculation.

The experimental programme comprised the testing ages of 12, 18, 36 and 84 h. For each age of testing, three monotonic tests and three cyclic tests were carried out. It is however remarked that the mentioned cyclic tests were always performed on the same three specimens: i.e., after being tested at the age of 12 h, the specimens were stored in the curing environment and re-tested at 18 h, 36 h and 84 h. This strategy was adopted because of the low levels of stress induced during the cyclic testing (1/3 of the tensile strength at the age of testing), which should not induce any kind of damage to the specimen and allow re-using it. Nonetheless, in order to confirm the feasibility of this re-utilization of specimens, three additional specimens were cast for cyclic testing solely at the age of 84 h from a virgin state. The comparison of results of testing of the three virgin specimens and the three re-used specimens at the age of 84 h can assist the assessment of the influence of the

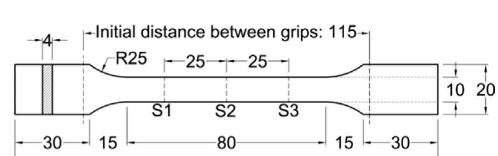

Fig. 1. Specimen dimensions according to ISO 527-2. Note: all dimensions are in millimetres.

loading history on the elasticity modulus. A specific nomenclature was devised for the test specimens, each one being labelled as X_Y_Z, where X is the test type (MTT – Monotonic tensile test, CTT – Cyclic tensile test), Y is the testing time in hours (12, 18, 36 and 84) and Z is the specimen number within the series. The summary of all tensile tests performed is shown in Table 1. It is remarked that CTT_84h_1 to CTT_84_3 correspond to the specimens that were re-used among the several testing ages, whereas CTT_84h_4 to CTT_84h_6 correspond to the specimens that were solely tested at such age (here termed as virgin specimens).

Both types of tensile tests (MTT and CTT) were carried out in a universal testing machine (AG-X Shimadzu) with 50 kN capacity load cell and test force measurement precision of 1/1000 $\pm$0.5%. A TML strain gauge (type: BFLA-5-3-3L; measuring length: 5 mm; gauge factor: 2.08 $\pm$1%) was installed on the top surface of each specimen (i.e. the surface that was bounded by the acetate sheet), at mid-length, to measure its longitudinal strain (see Fig. 2). The monotonic tensile tests were conducted under displacement control, at a rate of 1 mm/min, according to EN ISO 527-1:2012. In regard to the load configuration of cyclic tests, the testing protocol was inspired and adapted from existing standards for determination of static modulus of elasticity in compression of cement-based materials (ISO 1920-10:2010). Each CTT experiment was composed of six load/unload cycles between 10 N and the force corresponding to 1/3 of the average tensile strength of the specimen at the age of testing. The schematic representation of the test cycles is shown in Fig. 3. The cycles were generally performed under load control at the rate of 20 N/s, comprising 10 s long stretches of constant load upon reaching the maximum and minimum load values. The first loading was slightly different in the sense that was made with a constant displacement rate of 1 mm/min until the maximum load of testing was reached. This initial stretch of testing was performed under displacement control by reason of the machine operation and as to ensure the respect of the targeted stress limits. It is further remarked that the choice of a load rate of 20 N/s for the all ages of testing was based on the fatigue tests carried out by Shen et al. [18] and was related to the intent of matching the strain rate of the standard tensile tests for an intermediate value of stiffness of 4 GPa (1/2 of the expected ultimate value in the studied mix).

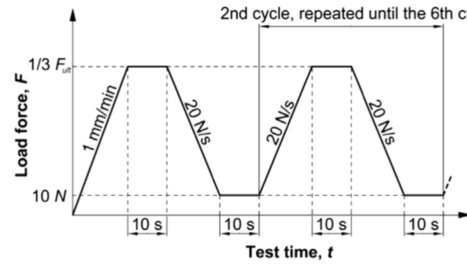

Fig. 3. Loading scheme of cyclic tests.

Table 1
Experimental programme of tensile tests.

Age	Series	Number of specimens	Test type	σ_{max}[a] [MPa]
12 h	MTT_12h	3	Standard	–
	CTT_12h	3	Cyclic	2.4
18 h	MTT_18h	3	Standard	–
	CTT_18h	3	Cyclic	4.7
36 h	MTT_36h	3	Standard	–
	CTT_36h	3	Cyclic	7.0
84 h	MTT_84h	6	Standard	–
	CTT_84h	6	Cyclic	7.0

[a] σ_{max}= 1/3 of ultimate strength.

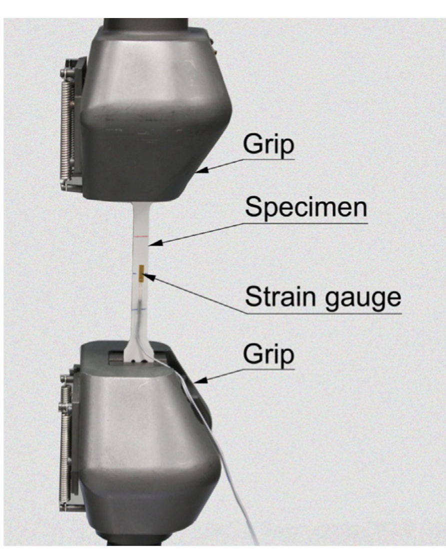

Fig. 2. Layout configuration of tensile tests.

2.2. EMM-ARM tests

The EMM-ARM is a variant of the traditional resonant frequency methods, based on the identification of the first flexural resonant frequency of a composite beam formed by a self-supporting mould filled with the material under testing. The natural frequency of the composite beam at each instant of testing can be analytically related to the *E*-modulus of the tested material, which allows determining the evolution of this elastic property since very early ages. In the original implementation of EMM-ARM for evaluating the stiffness evolution of concrete, the tested material was put inside an acrylic cylinder which was placed in simply supported condition [15]. Thereafter the methodology was adapted to study cement pastes by means of a smaller composite cantilever beam [16]. In order to adapt this ambient vibration technique to the study of epoxy adhesive used in FRP applications, some further alterations were necessary. Since the grain size of the filler of the epoxy (maximum grain size usually ranging between 0.2 and 0.5 mm [8]) is comparable to that of cement paste, it was decided to adopt a similar mould/strategy to the one used in EMM-ARM version applied to cement pastes, which is described in detail elsewhere [16]. Herein, focus will be addressed to essential aspects concerning the modified experimental setup, testing procedure and data acquisition.

The EMM-ARM experimental setup adopted for testing epoxy resin is reproduced in Fig. 4.

For specific details on this implementation and the corresponding procedure, see the work of Benedetti [19]. The mould consists of a 330 mm long acrylic tube, with internal and external diameters equal to 16 and 20 mm, respectively. This cross-sectional size respects the principle that the diameter of the beam should be at least 3–5 times larger than the nominal size of the particles of the tested material, in accordance to the criteria given by ASTM C192/C192M. Taking into account the extensive experience of the authors with this testing technique and bearing in mind the trade-off that exists between the decrease in specimen size and the corresponding increase in resonant frequencies (thus less excitable structures), it was decided to limit the maximum acceptable resonant frequency values of 80 Hz for the composite beam upon full hardening of the tested material ($\sim$8 GPa). The limitation of 80 Hz in the resonant frequency was associated to the intent of maintaining high excitability levels of the cantilever on behalf of ambient vibration, thus allowing this output-only modal identification technique to be applied with adequate robustness (i.e. clear

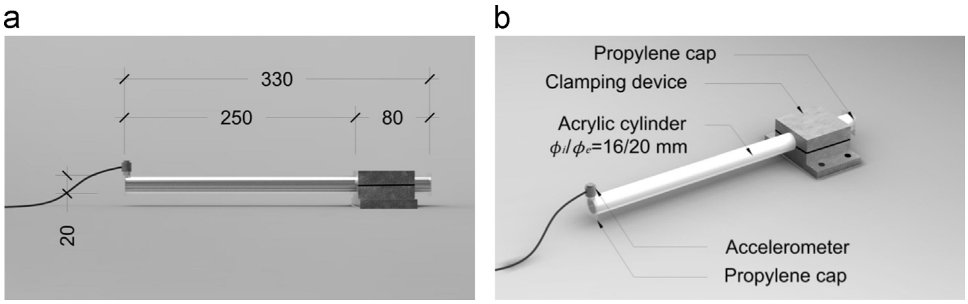

Fig. 4. Experimental setup of EMM-ARM tests: (a) geometry of the experimental setup (side view); and (b) components of the experimental setup. Note: all dimensions are in millimetres.

identification of resonant frequencies without needing complex data processing algorithms). In order to fulfil this requirement, the free span of the cantilever beam was set to 250 mm. It is stressed that the adopted geometry simultaneously allows the test to endure a significant variation range of resonant frequency of 50–80 Hz for a stiffening of the testing material from 0 to ~8 GPa. This wide range of frequency variation allows *E*-modulus evolution to be identified with a good resolution. A clamping device was used to assure complete fixation of the cantilever beam (see Fig. 4). This clamping system, tested for the first time in the work performed by Granja et al. [20], consisted of two steel parts fastened together with four screws and thus forming a central hole with a diameter equal to the outer diameter of the acrylic tube. It is noted that the clamping device itself was screwed to a heavy steel profile as to allow the consideration of perfect fixing of the cantilever.

In the EMM-ARM application for the study of cement pastes, the acrylic tube was already prepared with an extremity cap before the tube filling. In the present work, due to the higher viscosity of the epoxy adhesive after mixing, this was injected into the tube by using a 100 ml syringe, as shown in Fig. 5. This method of injection had already been successfully verified in preliminary tests, checking the possible formation of air bubbles inside the tested material due to a potentially inefficient injection of epoxy inside the mould.

When the tube was completely filled with the epoxy, two propylene lids were placed at both mould extremities. Finally, after putting the specimen in the final horizontal position, a ceramic shear piezoelectric accelerometer (PCB® Piezotronics 352C34, with mass of 5.8 g, sensitivity 100 mV/g; frequency range: 0.5–10,000 Hz) was placed at the free end of the cantilever, in order to monitor the accelerations of the extremity of the beam in the vertical direction. The beam is solely acted by its self-weight and ambient excitations that correspond to the vibrations that naturally occur in proximity of the experiment (e.g., people walking nearby; room ventilation; vibrations produced by mechanical equipment). These vibrations can conceptually be considered as a white noise, i.e. with a uniform energy content throughout the range of frequencies of interest. In order to increase the ambient vibration level, a domestic fan was used for blowing air to the EMM-ARM specimens. The monitoring procedures started immediately after the correct placement of all components, which occurred within ~20 min after mixing the epoxy adhesive.

Fig. 6 schematizes the necessary operations for obtaining the *E*-modulus evolution along time. The measured accelerations are acquired in a 24-bit data logger (NI-USB-9233) at a frequency (f_{acq}) of 500 Hz, and divided in sets of 300 s (Fig. 6a). Each recorded data set is converted to the frequency domain by applying Fast Fourier Transforms (FFT), using sub-sets of data with 4096 points (N_{FFT}) and Hanning windows with 50% overlaps, according to the Welch procedure [21]. It is thus possible to obtain the frequency response spectrum of the beam (Fig. 6b) for each 300 s period of testing with a frequency resolution (f_{res}) of 0.122 Hz (computed according

Fig. 5. Photo of the epoxy injection into the acrylic tube.

to Eq. (1)), where the peak corresponds to the resonant frequency of the system in such a time interval.

$$f_{res} = \frac{1}{2}\frac{f_{acq}}{N_{FFT}} \tag{1}$$

By identifying the highest peak in each amplitude spectrum, it is possible to obtain the resonant frequency evolution of the cantilever along time (see Fig. 6c).

The resonant frequency of the beam is finally related to the *E*-modulus of the tested material by application of the dynamic equations of the cantilevered structural system, together with the applied loads. The whole set of equations used for the characterization of *E*-modulus is explained in [16]. The final solution is the differential equation shown below

$$a^3\left[\cosh(aL)\cos(aL)+1\right]+\frac{w^2 m_p}{EI}\left[\cos(aL)\sinh(aL) - \cosh(aL)\sin(aL)\right]=0 \tag{2}$$

where $a=\sqrt[4]{w^2\times\overline{m}/EI}$, EI is the distributed flexural stiffness of the composite beam, $\overline{m}$ is the uniformly distributed mass per unit length, m_p is the concentrated mass at the free extremity of the cantilever (owing to the accelerometer and lid), L is the span of the cantilever, f is the first flexural resonant frequency, and $w=2\pi f$ is the corresponding angular frequency.

Therefore, for each measured frequency f it is possible to obtain the corresponding EI of the composite cantilever, and since the acrylic *E*-modulus E_a is known, Young's modulus of the tested epoxy adhesive E_e can be estimated through the following equation:

$$EI = E_a\frac{\pi(\varphi_e^4-\varphi_i^4)}{64}+E_e\frac{\pi\varphi_i^4}{64} \tag{3}$$

where φ_e and φ_i are the outer and inner diameters, respectively. In this way, it is possible to relate the evolution of the first natural frequency with the elastic modulus development during the testing time and to obtain plots of *E*-modulus versus time for the epoxy (Fig. 6d). This estimating methodology assumes that the fixed

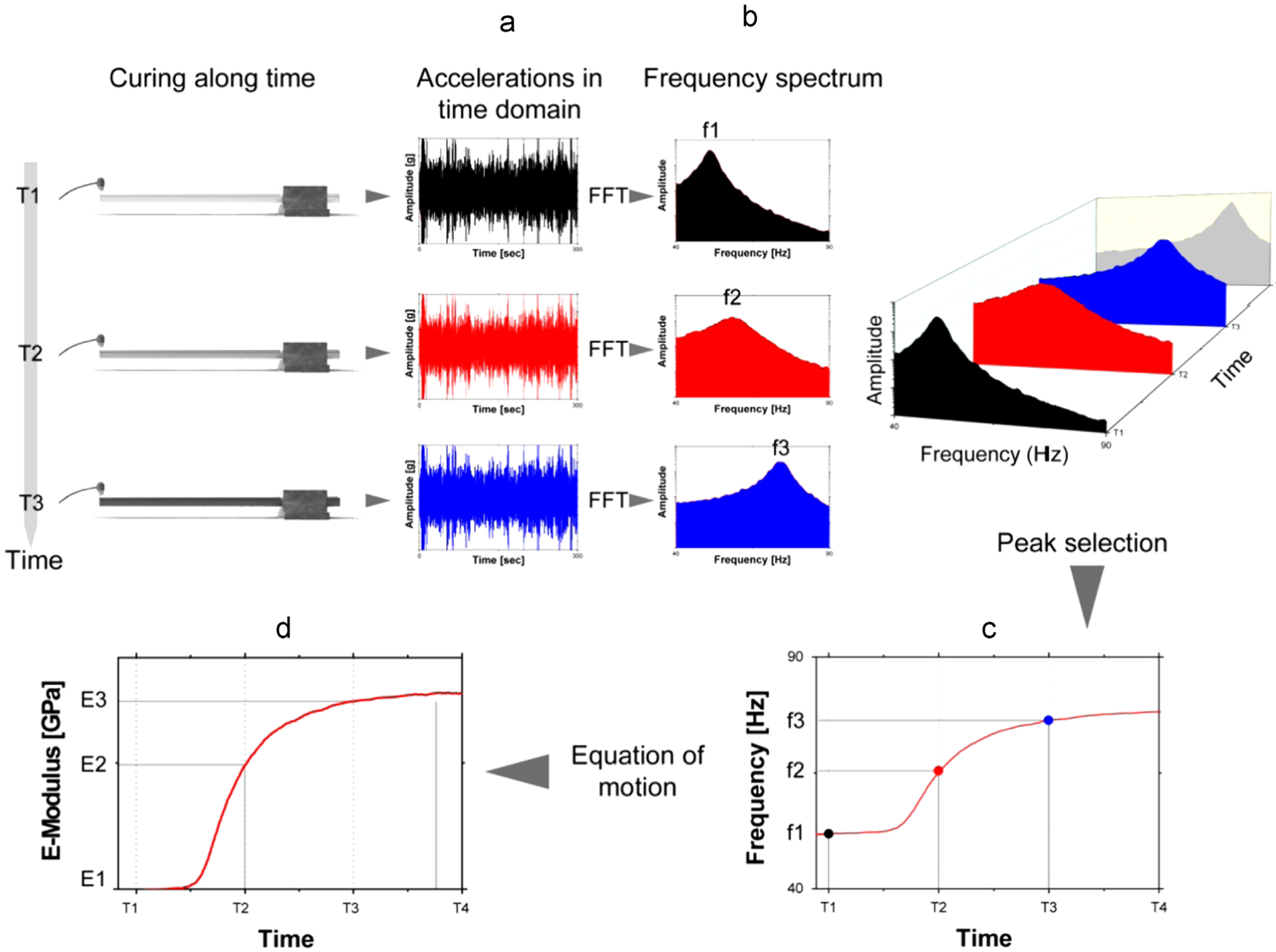

Fig. 6. EMM-ARM data processing scheme.

support of the cantilever is infinitely rigid and that the shear deformation and rotary inertia effects can be neglected. These assumptions were duly validated by parametric numerical analyses.

In order to check the method's ability to obtain results with good repeatability, two tests were performed simultaneously, using the same epoxy adhesive mixture employed for tensile tests. Table 2 shows the geometric characteristics of the used moulds, as well as the density of acrylic and epoxy adhesive. The values of *E*-modulus and density of the acrylic were verified in the laboratory through modal identification and weighing (with a Kern PLS 4000-2 precision balance 0.01 g: 4000 g) of the empty moulds before each test.

Table 2
Characteristics of EMM-ARM specimens.

Reference	L [mm]	φ_e [mm]	φ_i [mm]	m_p [g]	Acrylic density [kg/m^3]	Epoxy density [kg/m^3]
EMM1	250	20.15	15.99	12.11	1202.511	1742.935
EMM2	250	20.14	15.94	12.12	1198.909	1763.863

3. Results and discussion

3.1. Tensile tests results

Fig. 7 presents the stress–strain curves obtained at various ages by monotonic tensile tests. Stress was evaluated by dividing the applied load by the cross-sectional area of the specimen's mid-height section (where the strain gauge was placed). From this figure, it is possible to observe the increase on stiffness along the curing process of epoxy adhesive. At the age of 12 h, since the curing reactions had just begun, high values of strains were obtained. In fact, the monotonic tensile tests carried out at 12 h were stopped at about 5% strain (limit of the used strain gauges). From 12 to 36 h, the epoxy stiffness had a significant increase, shown by the strong slope difference of the curves obtained at 12, 18 and 36 h. From 36 to 84 h, the stress–strain curves did not exhibit any significant variation: in that period the average maximum tensile strength increased only of 0.2 MPa (1%). On the contrary, a decrease of 18% (0.0006 m/m) in ultimate strain was observed, confirming that curing reactions were still in progress between 36 and 84 h. The stress–strain curves obtained by cyclic tensile tests are depicted in Fig. 8. From this figure the same considerations made for monotonic tests results can be drawn: from 12 to 36 h after mixing of adhesive components, the material stiffness had an important increase, while, from 36 to 84 h, it did not show any significant variation. In addition, Fig. 8 clearly shows the viscoelastic effect that occurred during the consecutive loading/unloading cycles, especially at the early ages of testing. Furthermore, the strain–stress curves of the cyclic tensile tests concerning the additional three specimens tested just at the age of 84 h (from the virgin state), and those of the repeatedly tested specimens, turned out to be very similar. This confirms that loading history did not influence the material stiffness for the maximum load levels applied.

Young's modulus of epoxy adhesive was obtained by various methods. Concerning the monotonic tensile tests, two methods were contemplated: the first Young's modulus $E_{MTT\text{-}std}$ was calculated as the slope of the secant line between strain values of 0.05% and 0.25% on the stress–strain curve, in accordance to ISO standard 527-1; the second $E_{MTT\text{-}inslop}$ represents the slope of the linear trend line of the experimental values gathered until 1/3 of the ultimate strength, in accordance with the American Standard ASTM D638M-93. In order to avoid the error caused by the possible starting misalignment of the grips and the presence of microscopic structural flaws, the initial region of positive second derivative of each experimental curve was not considered for the calculation of $E_{MMT\text{-}inslop}$. The schematic representation of these two methods applied to the specimens MTT_18h_1 and MTT_84h_2 are shown in Fig. 9. The two calculation methods tend to lead to different values of E-modulus. Young's modulus values $E_{MTT\text{-}std,}$ were always lower than $E_{MTT\text{-}inslop}$ as shown in Fig. 10, where the evolution of the average values of E-moduli calculated through these two methods are depicted. Moreover, this difference depended on the age of the epoxy specimen and slightly decreased over time (in relative terms). At the age of 12 h, the average modulus calculated by the $E_{MTT\text{-}inslop}$ method resulted 49.3% larger than the secant modulus. At 84 h, an average E-modulus ($E_{MTT\text{-}std}$) of 7.16 GPa and an average $E_{MTT\text{-}inslop}$ of 9.39 GPa (31.3% larger) were obtained. This large deviation is not negligible and deserves a careful consideration. The modulus calculation laid down by ISO standard takes into account stretches of the stress–strain relationship curve where the slope of the obtained curve was not constant, as visible in the examples of Fig. 9 (MTT_18h_1 and MTT_84h_2). Furthermore, it should be noted that failure of MTT specimens tested at the age of 84 h

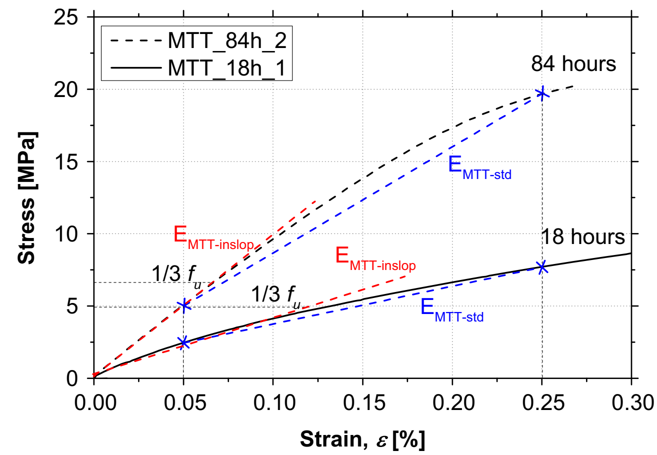

Fig. 9. Example of different methods of E-modulus calculation.

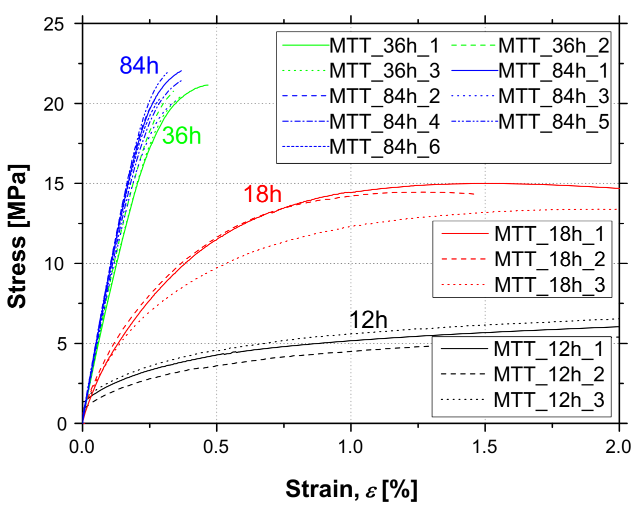

Fig. 7. Stress–strain curves obtained from monotonic tensile tests.

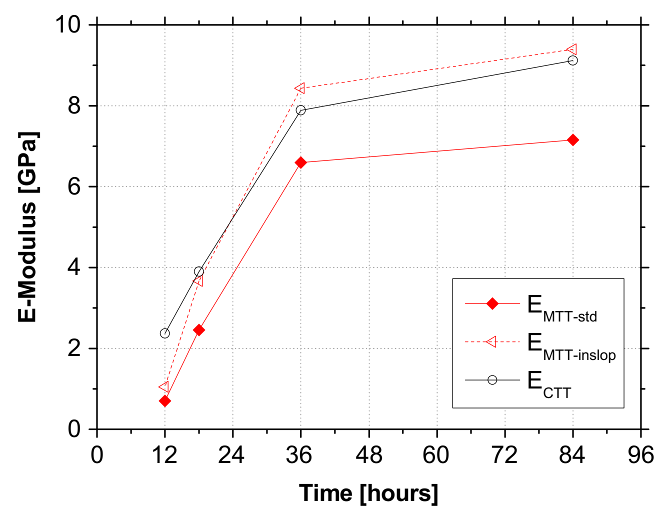

Fig. 10. Epoxy E-moduli evolution obtained by tensile tests.

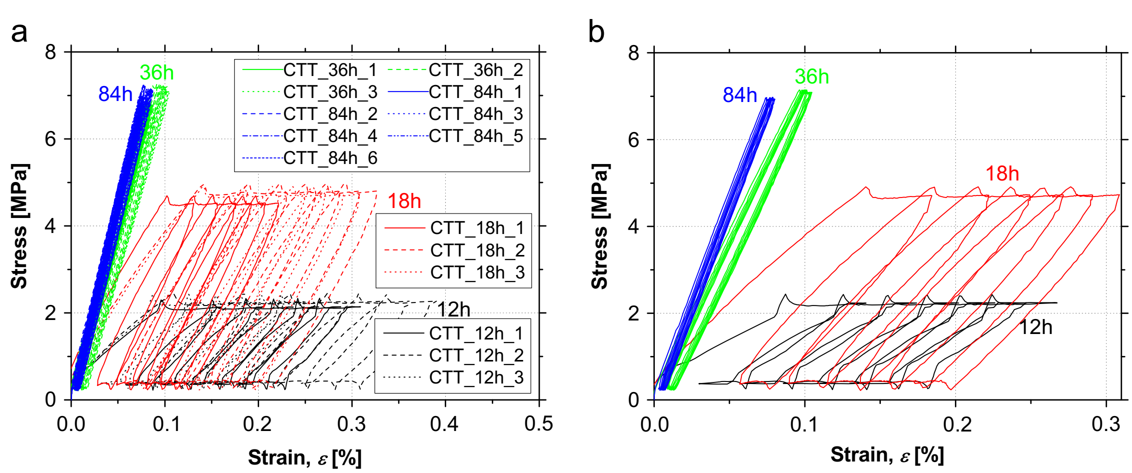

Fig. 8. Stress–strain curves obtained from cyclic tensile tests: (a) all specimens; and (b) one exemplifying specimen for each age.

occurred for a strain level of 0.27%, which is very close to 0.25%, thus probably inducing tensile damage to the specimen within this strain range. Conversely, the trend line method ($E_{MTT\text{-}inslop}$) takes into account values in the range of low strains for all ages of testing, where the relationship between stress and strain can be properly considered linear. Consequently, the elasticity modulus determined by ISO 527-1 equation ($E_{MTT\text{-}std}$) turned out to be systematically lower than that obtained through the trend line method ($E_{MTT\text{-}inslop}$). Moreover, the average coefficient of determination for the curves obtained by the trend line method ($R^2_{inslop}=0.9951$) resulted higher than that calculated for the ISO curves ($R^2_{std}=0.9579$). Thus $E_{MTT\text{-}inslop}$ approximates better the real data points, demonstrating that, in the considered range of values, the experimental curve is almost linear. This comparison confirms that standard recommendations may not estimate the actual stiffness of epoxy adhesive, since in the strain interval of 0.05–0.25% the material may have an inelastic behaviour, especially at early ages.

The aforementioned *E*-modulus values computed with basis on the results of standard tensile test setups/procedures (with calculation methods $E_{MTT\text{-}std}$ and $E_{MTT\text{-}inslop}$) are now compared to those that can be obtained from the tensile cyclic tests results. Concerning the latter, the first cycle of loading was neglected and the slope of the trend line calculated for each following loading and unloading stage was taken into account for determining *E*-modulus values. Fig. 11 shows the strain–stress curves obtained in a cyclic test carried out at the age of 84 h (CTT_84h_3). Based on this figure and Table 3, some considerations can be drawn: (i) the slopes corresponding to each loading and respective unloading stage resulted very similar; (ii) a relevant coherence between slopes pertaining to the five different subsequent cycles was obtained. Therefore it is feasible to average all these slopes within each test to obtain a representative *E*-modulus of the cyclic test (E_{CTT}). It was also noticed that the dispersion of results among the five test cycles tends to decrease with increasing ages of testing.

The evolution of the average elasticity moduli evaluated according to the cyclic tensile test methodology (CTT) is shown in Fig. 10, together with the previous two methodologies. It is interesting to observe that the coherence between CTT tests results (E_{CTT}) and those obtained through the trend line method on the MTT tests ($E_{MTT\text{-}inslop}$) is quite satisfactory, particularly for the ages 18 and 84 h. However, for all the tested ages the ISO calculation method ($E_{MTT\text{-}std}$) identifies much lower values for the adhesive *E*-modulus when compared to the other methodologies, with differences that range from −70.4% to −22.1% during the several testing ages.

3.2. EMM-ARM tests results

The frequency spectra obtained for specimen EMM2 at several ages are shown in Fig. 12. From this figure, it is possible to clearly identify the resonant frequency at the depicted ages, since the peaks are easily recognizable and no significant secondary peaks emerge in the frequency range of interest. If all computed power spectra are put side by side according to their time of occurrence, a meaningful 2D colour plot may be obtained, in which the intensity of the signal is revealed by colour scale, as shown in Fig. 13. For each test, the curves of first natural frequencies versus time are identified, taking the peak of each power spectrum. The resonant frequencies evolution obtained for the two specimens are shown in Fig. 14. It is remarked that the two frequency curves are very coherent, providing an indication of good repeatability of the experimental setup and procedures. Moreover, a wide range of frequencies was covered throughout the curing process of the epoxy adhesive, ranging from 51.3 Hz to 79.6 Hz within the testing period; *E*-modulus evolution can thus be identified with a good resolution (0.034 GPa for 51.3 Hz and 0.052 GPa for 79.6 Hz). The frequency evolution curves appear to be plausible, showing an initial period of approximately 6.4 h in which the frequency remains almost constant. After this threshold, the frequencies evolved significantly for both tested specimens until approximately 36 h of curing. After such period, the slope of variation

Table 3
Summary of tests results.

Age	Reference	$E_{5cycles}$ [GPa]	CoV [%]	Reference	$E_{MTT\text{-}std}$ [GPa]	$E_{MTT\text{-}inslop}$ [GPa]	EMM_{avg} [GPa]
12 h	CTT_12h_1	2.32	8.96	MTT_12h_1	0.70	1.08	6.01
	CTT_12h_2	2.27	10.17	MTT_12h_2	0.66	0.93	
	CTT_12h_3	2.53	7.94	MTT_12h_3	0.74	1.14	
18 h	CTT_18h_1	4.24	4.63	MTT_18h_1	2.55	3.57	8.23
	CTT_18h_2	3.75	6.29	MTT_18h_2	2.62	3.83	
	CTT_18h_3	3.71	5.83	MTT_18h_3	2.18	3.61	
36 h	CTT_36h_1	8.20	0.66	MTT_36h_1	6.44	8.27	9.41
	CTT_36h_2	8.04	0.98	MTT_36h_2	6.84	8.81	
	CTT_36h_3	7.42	0.72	MTT_36h_3	6.50	8.21	
84 h	CTT_84h_1	9.36	0.29	MTT_84h_1	7.36	9.59	9.69
	CTT_84h_2	9.17	0.20	MTT_84h_2	7.27	9.87	
	CTT_84h_3	8.71	0.41	MTT_84h_3	6.68	8.93	
	CTT_84h_4	8.85	0.30	MTT_84h_4	6.99	8.97	
	CTT_84h_5	9.44	0.21	MTT_84h_5	7.54	9.59	
	CTT_84h_6	9.19	0.29	MTT_84h_6	7.11	9.43	

Notes: $E_{5cycles}$ = average *E*-modulus of five loading cycles; CoV = coefficient of variation; EMM_{avg} = average of *E*-modulus values obtained by EMM-ARM.

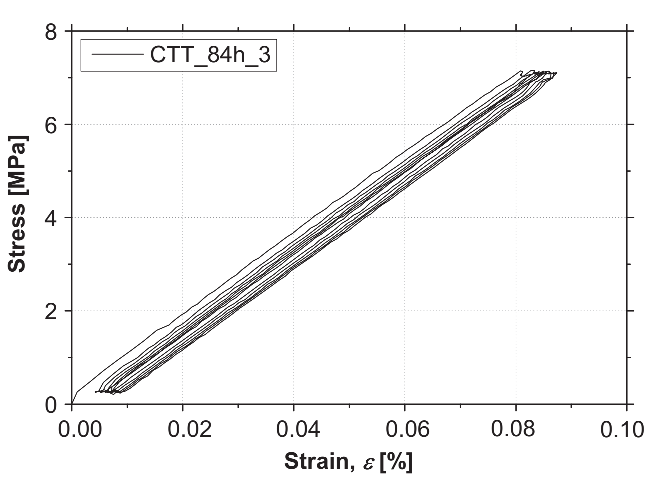

Fig. 11. Example of stress–strain curve obtained from cyclic test at 84 h.

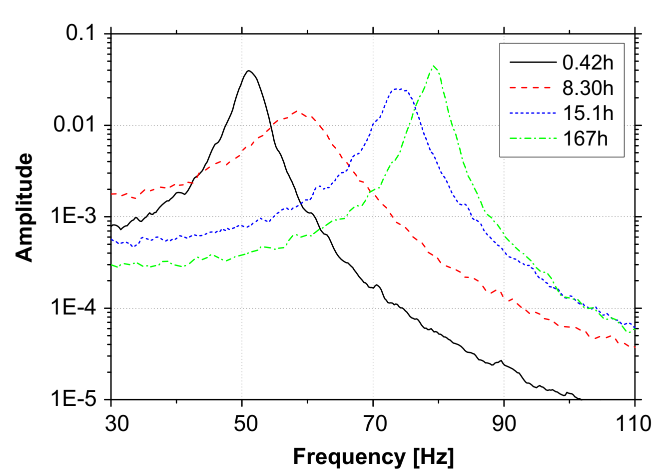

Fig. 12. Frequency spectra for EMM-ARM beam EMM2 at different ages.

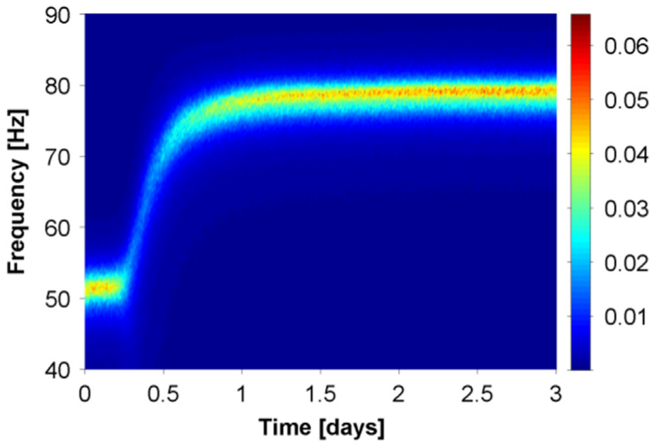

Fig. 13. Colour map of measured frequency spectra along time for the specimen EMM2. (For interpretation of the references to colour in this figure legend, the reader is referred to the web version of this article.)

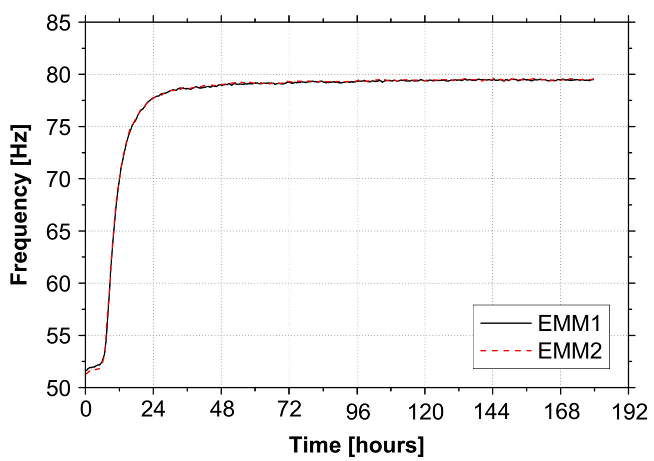

Fig. 14. Resonant frequency evolution of the EMM-ARM beams.

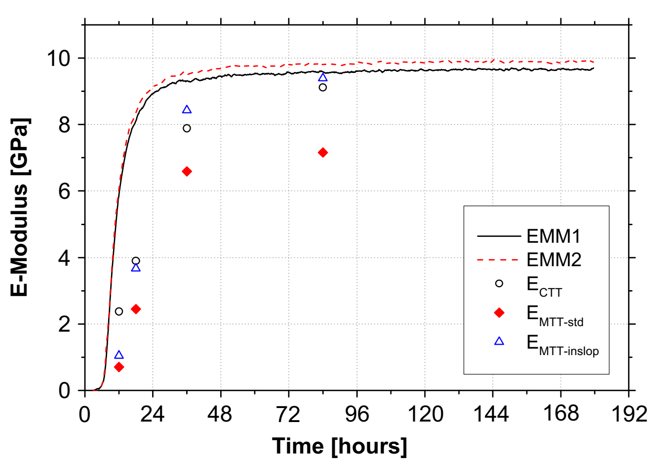

Fig. 15. *E*-modulus evolution obtained by EMM-ARM, MT and CT tests.

exhibits a significant decrease. The elasticity modulus of the tested epoxy adhesive mixture was estimated by applying Eqs. (2) and (3). The stiffness evolution for both EMM-ARM specimens is shown in Fig. 15. It is noted that based on the adopted test setup (sizes, stiffnesses and weights) and the frequency resolution mentioned above, the *E*-modulus minimum resolution is 0.05 GPa. The agreement between the results of the two specimens is very good, with absolute stiffness differences under 2.5% (0.22 GPa at the age of 168 h), demonstrating adequate repeatability of EMM-ARM. In the initial period (during the first ~6.4 h) the epoxy adhesive stiffness was nearly null for both specimens, which is consistent with its fluid-like behaviour. The kinetics of evolution of *E*-modulus was consistent with the one already described and discussed for the frequency evolution, and the final reached value at the end of testing was 9.3 GPa/9.5 GPa for EMM1/EMM2.

3.3. Comparison between EMM-ARM, MTT and CTT results

Fig. 15 also shows the comparison between the elastic modulus results obtained by EMM-ARM and by tensile test methods (monotonic and cyclic). At the age of 84 h, there is a good agreement between the values obtained through the EMM-ARM (EMM1 and EMM2), those collected in cyclic tests (E_{CTT}) and those calculated from the initial slope of monotonic stress–strain curves ($E_{MTT\text{-}inslop}$). However, the results show relevant differences at the earlier ages of 12, 18 and 36 h. At such ages, all the *E*-modulus values obtained from tensile tests are significantly lower than the ones acquired from EMM-ARM, particularly at 12 and 18 h. This deviation may be explained by different time-scales and strain-rates of the experimental tests. However, the strain-rate of the different methods, ranging between 10 and 50 με/s for EMM-ARM (computed through numerical integration of the accelerograms) and between 100 and 110 με/s for the monotonic tensile tests (computed directly from the strain measurements) are within the same order of magnitude and therefore are not different enough to justify the gap between the estimated *E* values. Nevertheless, the EMM-ARM has a much lower period of loading (within a range of 0.016 and 0.02 s) than the monotonic tensile tests (within a range of 10 and 20 s). This lower time-scale makes the method less sensitive to the viscoelasticity of the material.

Fig. 16 presents the strain–time curves obtained in two exemplifying tests performed at the age of 18 and 84 h. From this figure, it is possible to observe the increase of strain during the 10 s intervals in which the load remained constant. This increase was significantly evident at the earlier age, while it was much more attenuated at 84 h. Moreover, a progressive accumulation of deformation while material was subjected to cyclic loading was verified. In fact, the peak strain increased with the increasing numbers of cycles. At the age of 18 h, an increase of 73.9% in maximum strain between the first and the last cycle was obtained (Fig. 16a). At the age of 84 h, the accumulated strain after six cycles turned out to be very lower (5.3% of the initial maximum strain), as shown in Fig. 16b. This process of a continuous increase in strain is called cyclic creep (or ratcheting strain) [18] and it confirms that epoxy resin shows a typical visco-elastic behaviour. Therefore, the high visco-elasticity that epoxy exhibited at very early ages may have influenced the measurement of elastic modulus through tensile tests, leading to lower values. As the importance of creep strains decreased over curing time, Young's modulus obtained by quasi-static tests got closer to the actual *E*-modulus.

4. Conclusions

The present paper aimed to assess the early-age development of stiffness of an epoxy adhesive used in FRP strengthening applications, by means of three test methodologies: EMM-ARM, ISO standard monotonic tensile tests and cyclic tensile tests. The analysis of the obtained experimental results led to the following main conclusions:

(1) During the entire tensile cycling process, the slope of the elastic loading and unloading did not decrease, i.e. the calculated *E*-modulus values were very similar for all the cycles. Moreover, coherence between Young's moduli determined

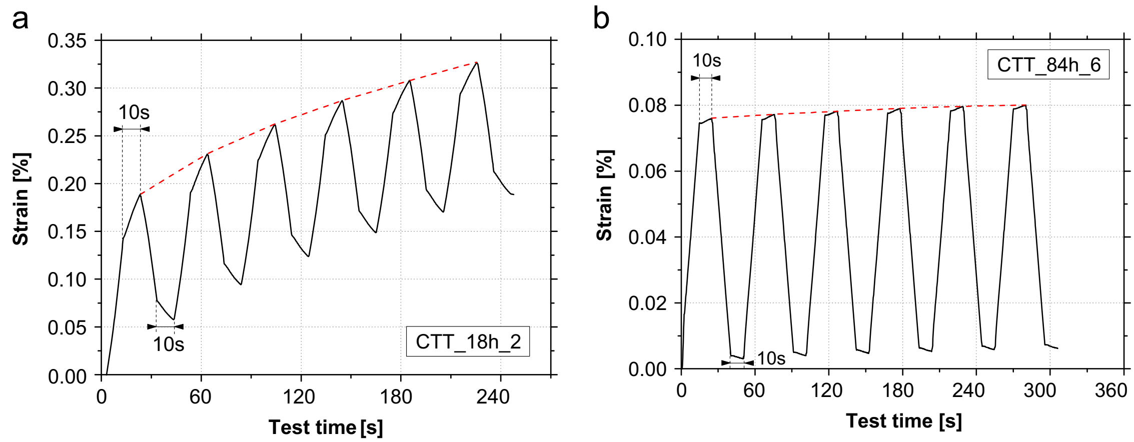

Fig. 16. Strain evolution along testing time at: (a) 18 h; and (b) 84 h.

through cyclic tests and those obtained from monotonic tests by taking into account the initial slope of the stress–strain response was observed.

(2) The method for calculation of *E*-modulus provided by ISO 527:1:2012 led to lower values of the elasticity modulus for the tested epoxy resin, due to the fact that, in the considered strain interval (0.05–0.25%), the stress–strain relationship of the adhesive was non-linear. Since the non-linear mechanical behaviour of epoxy adhesive is further marked at very early ages, it is clear that ISO method leads to even higher deviations (as compared to the other methods described here) for determining the epoxy resin *E*-modulus at the early stage of curing process. Therefore, a linear regression procedure applied on the part of the stress–strain curve corresponding to the values gathered until 1/3 of the ultimate strength is considered recommendable. In fact, at the indicated lower stress range, the stress–strain relationship can be considered linear.

(3) The EMM-ARM technique revealed its capability in clearly identifying the hardening kinetics of epoxy adhesives, measuring the material setting time and the stiffness growth since very early ages. This method allows measurements since the tested material still has 'fluid-like' behaviour, overcoming the main drawback of the traditional resonance methods.

(4) The results obtained by EMM-ARM were compared with the outcome of tensile tests. Quasi-static tests provided values of Young's modulus that were lower than the values collected by EMM-ARM. This difference can be explained by the significant visco-elastic behaviour that epoxy resin exhibits especially at very early ages. In fact, this difference significantly decreased as the epoxy adhesive hardened, becoming negligible at the age of 84 h.

Acknowledgements

This work is supported by FEDER funds through the Operational Program for Competitiveness Factors – COMPETE and National Funds through FCT – Foundation for Science and Technology under the projects CutInDur PTDC/ECM/112396/2009 and VisCoDyn EXPL/ECM-EST/1323/2013. The authors also like to thank all the companies that have been involved supporting and contributing for the development of this study, mainly, S&P Clever Reinforcement Ibérica Lda. and Vialam – Indústrias Metalúrgicas e Metalomecânicas, Lda. The first and second authors acknowledge the grants SFRH/BD/80682/2011 and SFRH/BD/80338/2011, respectively, provided by FCT.

References

[1] Dunn DJ. Engineering and structural adhesives. Shropshire, UK: Rapra Technology; 2004.
[2] ACI. 440.2R-08 guide for the design and construction of externally bonded frp systems for strengthening concrete structures. Farmington Hills, USA: American Concrete Institute; 2008. p. 76.
[3] De Lorenzis L, Teng JG. Near-surface mounted FRP reinforcement: an emerging technique for strengthening structures. Compos B: Eng 2007;38:119–43.
[4] Gillham JK. Formation and properties of thermosetting and high T_g polymeric materials. Polym Eng Sci 1986;26:1429–33.
[5] Czaderski C, Martinelli E, Michels J, Motavalli M. Effect of curing conditions on strength development in an epoxy resin for structural strengthening. Compos B: Eng 2012;43:398–410.
[6] Matsui K. Effects of curing conditions and test temperatures on the strength of adhesive-bonded joints. Int J Adhes Adhes 1990;10:277–84.
[7] Lapique F, Redford K. Curing effects on viscosity and mechanical properties of a commercial epoxy resin adhesive. Int J Adhes Adhes 2002;22:337–46.
[8] Moussa O, Vassilopoulos AP, de Castro J, Keller T. Early-age tensile properties of structural epoxy adhesives subjected to low-temperature curing. Int J Adhes Adhes 2012;35:9–16.
[9] Michels J, Sena-Cruz J, Czaderski C, Motavalli M. Structural strengthening with prestressed CFRP strips with gradient anchorage. Compos Constr 2013;17:651–61.
[10] Tognana S, Salgueiro W, Somoza A, Marzocca A. Measurement of the Young's modulus in particulate epoxy composites using the impulse excitation technique. Mater Sci Engin A 2010;527:4619–23.
[11] Deng S, Hou M, Ye L. Temperature-dependent elastic moduli of epoxies measured by DMA and their correlations to mechanical testing data. Polym Test 2007;26:803–13.
[12] Yu H, Adams RD, da Silva LFM. Development of a torsion pendulum and its application to measuring the dynamic modulus of adhesives from pre-gelation to the cured state. Meas Sci Technol 2014;25:055603.
[13] Frigione M, Maffezzoli A, Acierno D, Luprano VAM, Montagna G. Nondestructive and in-situ monitoring of mechanical property buildup in epoxy adhesives for civil applications by propagation of ultrasonic waves. Polym Eng Sci 2000;40:656–64.
[14] Summerscales J. Non-destructive testing of fibre-reinforced plastics composites. Cambridge, UK: Springer; 1990.
[15] Azenha M, Magalhães F, Faria R, Cunha Á. Measurement of concrete *E*-modulus evolution since casting: a novel method based on ambient vibration. Cem Concr Res 2010;40:1096–105.
[16] Azenha M, Faria R, Magalhães F, Ramos L, Cunha Á. Measurement of the *E*-modulus of cement pastes and mortars since casting, using a vibration based technique. Mater Struct 2012;45:81–92.
[17] S&P, S&P resin 220 epoxy adhesive, Saftey data sheet; 2011, p. 6.
[18] Shen X, Xia Z, Ellyin F. Cyclic deformation behavior of an epoxy polymer. Part I: experimental investigation. Polym Eng Sci 2004;44:2240–6.
[19] Benedetti A. A new method for continuous quality control of NSM CFRP systems, [MSc thesis]. Bologna, Italy: School of Engineering and Architecture, University of Bologna; 2014.
[20] Granja J, Azenha M, Sousa Cd, Ferreira C. Comparison between different experimental techniques for stiffness monitoring of cement pastes. J Adv Concr Technol 2014;12:46–61.
[21] Welch PD. The use of fast Fourier transform for the estimation of power spectra: a method based on time averaging over short, modified periodograms. IEEE Trans Audio Electroacoust 1967;15:70–3.